Application of burnable absorbers in an accelerator driven system

Jan Wallenius, Kamil Tuček, Johan Carlsson, Waclaw Gudowski
Department of Nuclear & Reactor Physics
Royal Institute of Technology
100 44 Stockholm, Sweden
E-mail: janne@neutron.kth.se

Abstract

The application of burnable absorbers (BA) for minimization of power peaking, reactivity loss and capture to fission probabilities in an accelerator driven waste transmutation system (ADS, ATW) has been investigated. ^{10}B enriched B_4C absorber rods were introduced into a lead/bismuth cooled core fuelled with TRU discharges from light water reactors in order to achieve smallest possible power peakings at a BOL sub-criticality level of 0.97. Detailed Monte Carlo simulations show that a radial power peaking equal to 1.2 at BOL is attainable using a four zone differentiation in BA content. Using a newly written Monte Carlo Burnup code (MCB), reactivity losses were calculated to be 640 pcm per percent transuranium burnup, for unrecycled TRU discharges. Comparing to corresponding values in BA free cores, BA introduction diminishes reactivity losses in TRU fuelled sub-critical cores by about 20%. Radial power peaking after 300 days of operation at 1200 MW thermal power was less than 1.75 at a sub-criticality level of ~ 0.92, which appears to be acceptable, with respect to limitations in cladding and fuel temperatures. In addition, the use of BA yields significantly higher fission to capture probabilities in even neutron number nuclides. Fission to absorption probability ratio for ^{241}Am equal to 0.33 was achieved in the configuration here studied. Hence, production of the strong α-emitter ^{242}Cm is reduced, leading to smaller fuel swelling rates and pin pressurization. Disadvantages following BA introduction, such as increase of void worth and decrease of Doppler feedback in conjunction with small values of β_{eff}, need to be addressed by detailed studies of sub-critical core dynamics.

Introduction

As was shown in studies made at CEA, recycling of both plutonium, americium *and* curium is mandatory in order to achieve a substantial reduction factor ($\sim$ 100) of the radiotoxic inventory sent to geological repository from present nuclear parks [1]. The introduction of a major fraction of minor actinides into the nuclear fuel cycle however raises complex issues regarding reprocessing, fuel fabrication, core behaviour during transients and fuel performance during irradiation. In general, it is assumed that americium (and curium) is to be recycled in fast reactors, due to the superior neutron economy of the fast neutron spectrum, which will allow for higher burnups, and hence lower losses to secondary waste streams.

One option being considered for the minor actinide (MA) management is burnout in a second stratum of "dedicated" actinide burner reactors [2, 3]. As the vanishing Doppler feedback in conjunction with a very low β_{eff} would lead to deterioration of safety margins for critical configurations, sub-critical designs have been adopted for these MA-burners by a number of authors [4, 5, 6, 7].

Excess plutonium from light water reactors may be recycled in fast reactors. Homogeneous mixing of Pu with the minor actinides in accelerator driven systems (ADS) has also been proposed [8, 9, 10]. Since requirements on Doppler feedback are relaxed, the ADS core spectrum can be much harder than for corresponding critical configurations [11, 12, 13]. Consequently, americium and curium production in the entire fuel cycle is minimised. A major drawback of this approach is the large reactivity loss appearing due to burnout of ^{239}Pu and ^{241}Pu, with a concomitant increase in power peaking that may not easily be compensated for by a change in accelerator proton current. Consequently, maximum burnup becomes limited by power peaking factors, rather than by radiation damage to cladding and fuel.

The introduction of thorium as a fertile material to keep up reactivity [9] would imply the implementation of an entire new fuel cycle, and must be regarded as a distant future option. The application of burnable absorbers to perform the same task has to the authors' knowledge not received much attention in the published literature, apart from the suggestion to use ^{99}Tc in-core sub-assemblies [10]. Hence we have performed an investigation of advantages and drawbacks resulting from a massive introduction of classical burnable absorbers in sub-critical TRU-fuelled cores. First we show how power peakings can be minimised by use of a differentiated concentration of neutron absorbers in a lead/bismuth cooled core. Then, burnup calculations reveal the impact of the BA introduction on reactivity losses and effective minor actinide destruction rates. Finally we discuss how the design can be further improved.

System concept

The burnable poison option was considered for the CAPRA design [11], in order to cope with the high Pu reactivity. The option was however rejected due to degradation of reactivity coefficients needed for safe operation of a critical reactor. On the other hand, in a sub-critical system, one may have enough criticality margin in order to accommodate a positive void coefficient in conjunction with vanishing Doppler feedback. In addition, the absorber will have a positive influence on transmutation efficiencies in terms of fission to absorption ratios, since they shield slower neutrons from being captured by even neutron number TRU nuclides.

While already having introduced BA into the core, a differentiated concentration could be used for flattening of the core's power density distribution. As it turns out, radial power peakings at BOL can be virtually eliminated by an appropriate distribution of absorber pins among the fuel pins in each sub-assembly. Since the absorbers should be burnable, we have chosen enriched boron carbide as a reference material. Boron carbide is used in FBR control rods due to its high reactivity worth in fast neutron spectra.

Since sub-criticality is assumed, an additional cost is to be paid in terms of spallation neutrons to initiate the fission cascade. In order to maintain a high multiplication of source neutrons during burnup we substitute the absorber matrix in the inner core zones with depleted uranium, which also is more tolerant to increase in power peaking. Obviously, this diminishes effective TRU transmutation rates somewhat.

Even with a successful power flattening strategy implemented at BOL, power peaking will increase with burnup in sub-critical systems, as neutron multiplication decreases. Since power densities are limited by linear ratings, the number of fuel pins and consequently the number of dedicated cores needed to manage the minor actinides will depend on choice of fuel matrix and coolant. In the present study we have adopted nitride fuels, which may enable a doubling of linear ratings, as compared to the corresponding uranium free oxide and metal fuels.

Expected problems with high temperature stability of nitride fuels may be addressed by use of nitrogen bonding, which is known to suppress decomposition of actinide nitrides up to temperatures of 2800 K [14, 15]. Production of ^{14}C may be minimised by usage of 99% ^{15}N enriched nitrogen, today available on a commercial basis.

We have chosen lead/bismuth as a coolant in our present simulations, in order to mitigate the increase in void worth due to massive BA presence in the core. The spallation target was also set to be liquid/lead bismuth, in accordance with European ADS project preferences.

One purpose of our design study is to show how one may avoid americium production during the transmutation of transuranics nuclei. Thus the composition of TRU vector, exhibited in Table 1, was assumed to be that of typical un-recycled PWR spent fuel 30 years after discharge (which may be a reasonable value for the ADS introduction time delay). This vector differs from the one assumed for

Isotope	Mass fraction
^{237}Np	0.049
^{238}Pu	0.019
^{239}Pu	0.494
^{240}Pu	0.217
^{241}Pu	0.033
^{242}Pu	0.062
^{241}Am	0.108
^{243}Am	0.016
^{244}Cm	0.002

Table 1: TRU vector of the fuel used in the present study. The composition represents the TRU discharge of an average PWR after a burnup of 40 GWd/t and 30 years of cooling.

the CAPRA design, i.e. a mixture of Pu from fresh PWR discharges and recycled CAPRA plutonium [16]. The core design is hence to be regarded as a start-up configuration in a two-component scenario [6]. It is true that the Pu vector in a plutonium *only* recycling scheme reaches equilibrium within 25 years, [16]. However, adding the inevitable americium recycling, the appearance of (quasi) equilibrium TRU vectors is delayed by another 50 years [17, 9], and therefore we find it relevant to start by investigating requirements for start-up cores.

Core design

Figure 1 shows the geometry of our preliminary core design. The core is baptized to the "Sing Sing Core" (SSC), alluding to Swedish laws on reactor design. The fuel assembly duct flat to flat distance was taken to be 22.0 cm. The radius of our spallation target then becomes 24.9 cm, with a five mm thick steel container enclosing the target circuit. The active core height is assumed to be 100 cm, with proton beam impact located 18 cm above mid plane.

The choice of lead/bismuth as a coolant leads to certain constraints on sub-assembly designs, required for avoiding problems with corrosion of clad and structural material: Pitch to pin diameter ratios have to be comparatively large, to compensate for limitations in Pb/Bi flow velocities ($v <$ 3.0 m/s) imposed by erosion rates of cladding protective oxide films [18]. Pellet, pin and assembly dimensions were configured to keep outer cladding temperatures below 600 degrees C in the hottest channel at EOL and are displayed in Tables 2 and 3. Technetium and burnable absorber pellets have the same diameter as the the fuel pellets, but come without the central hole.

Modelling tools

We have applied continuous energy Monte Carlo simulation methods to all aspects concerning neutronics and burnup modelling of the Sing Sing Core. The JEF2.2 neutron cross section library was processed with NJOY [19] to create Doppler broadened pointwise cross section files for MCNP [20] in the temperature range 300 K to 1800 K. A three dimensional geometry setup was constructed, where all 84 fuel bundles of the core were modelled separately. Duct walls were explicitly present, while a smeared coolant/cladding/fuel material composition was used for the duct interior in most cases. MCNP4C with explicit delayed neutron transport was used to obtain *k*-eigenvalues and β_{eff}, while MCNPX [21] in proton source mode was applied to all calculations of neutron fluxes, power densities, cross sections, and neutron life times at BOL. A pin by pin model was used to calculate the relative fraction of heat deposition in cladding and coolant.

Burnup calculations were made with MCB, a continuous energy Monte Carlo Burnup code being developed at KTH

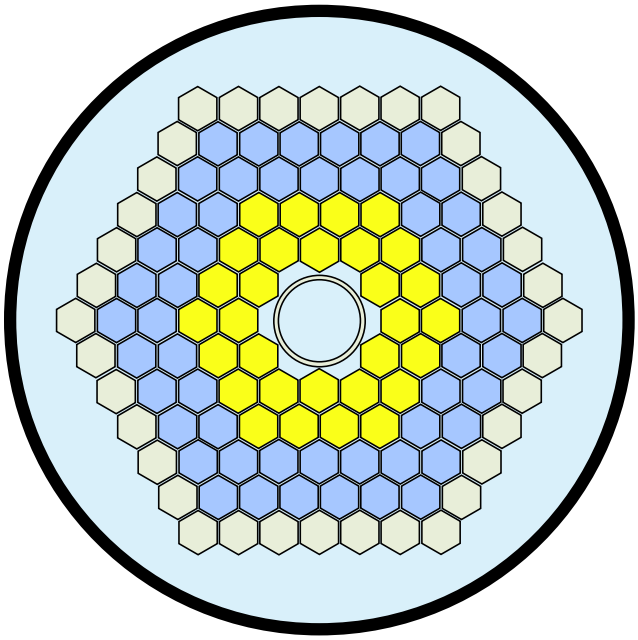

Figure 1: Cross section of the Sing Sing Core. 84 hexagonal fuel assemblies with duct flat to flat distances of 22.0 cm are configured in four fuel zones containing variable concentrations of TRU, depleted uranium (yellow zones) and boron carbide (blue zones). Technetium pins are present in zone two, and grey denotes steel reflector assemblies.

Property	Value
Active pin length	100 cm
Pellet inner radius	1.00 mm
Pellet outer radius	2.40 mm
Clad inner radius	2.49 mm
Clad outer radius	2.94 mm
Fuel density	0.90 TD
Smear density	0.70 TD

Table 2: Pin and pellet design parameters of the lead/bismuth, nitride fuelled Sing Sing Core.

in cooperation with AGH in Cracow [22, 23]. MCB extends MCNP with *internal* modules for reaction rate and heating calculations *in flight*. MCNPX was used to write a low energy (E $<$ 20 MeV) neutron source on the surface of the spallation target, that was employed for the burnup calculations with MCB. The effect of neglecting the high energy tail of spallation neutrons (1.4% of the source flux entering the core) was estimated to be within Monte Carlo error bars for power densities and actinide burnup.

Absorber introduction

The absorber ideally should serve the multifold purpose of neutron capture shielding, power peaking flattening, and mitigation of reactivity loss. While other materials like hafnium and europium are good absorbers in a fast neutron spectrum, they are not burnable as boron is. Employing 95% ^{10}B enriched B_4C, neutron moderation as well as absorber inventory is minimized. Figure 2 displays the absorption cross section of ^{10}B superimposed on the capture and fission cross sections of ^{241}Am. It is evident that an enriched boron carbide environment may suppress production rates of ^{242}Cm, while only affecting ^{241}Am fission rates to a minor extent.

Thus, boron carbide pins were introduced into fuel zones 3 and 4 in proportions yielding the flattest possible power distribution at BOL. Depleted uranium replaced the absorber in zone 1 and 2, in order to improve spallation neutron multiplication. Finally, technetium pins were positioned in zone 2, for transmutation purposes.

Table 4 shows a distribution (relative volume fraction) of transuranium nitride, uranium nitride and BA yielding a BOL radial power peaking equal to 1.2. The resulting radial power density along the symmetry axis of the core is displayed in Figure 3. Evidently, power peakings similar to those of critical reactor cores are feasible in subcritical systems.

The capture of slower neutrons in absorber rods placed in direct conjunction to fuel rods leads to suppression of the low energy part of the neutron spectrum in the fuel. By introducing the absorber pins directly in fuel assemblies instead of having them in separate fuel bundles (FBR approach), one avoids local flux suppression and is able to utilize the full reactivity worth of the absorber. Figure 4 exhibits the impact of the high boron carbide concentration in

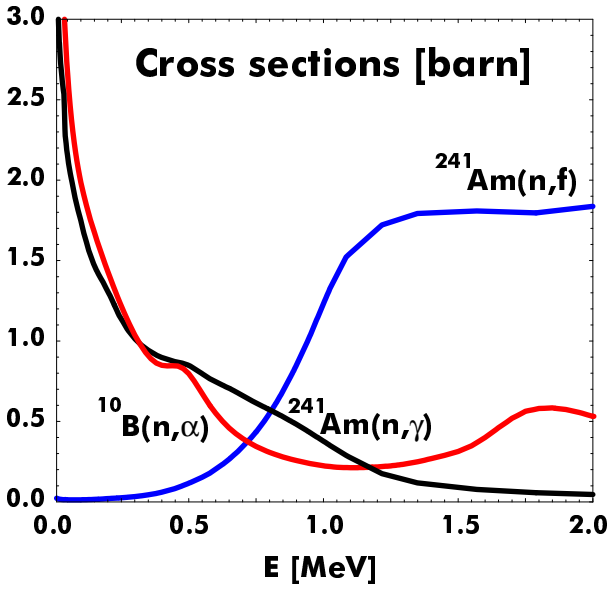

Figure 2: Absorption cross section of ^{10}B, compared to the capture and fission cross sections of ^{241}Am. For high ^{10}B concentrations in fuel bundles, neutron capture in ^{241}Am will be suppressed below 500 keV, without significant deterioration of ^{241}Am fission probabilities.

the outer fuel zones. While the magnitude of the neutron flux above the fast fission threshold ($E_n > 1$ MeV) is similar in zones one and three, a suppression factor larger than three is achieved in the resonance region ($E_n < 100$ keV).

The variation in neutron spectrum over the core is further characterized in Table 5, where median and flux weighted neutron energies are given for each fuel zone.

Comparing with the pin data given in Table 4 it is clear that a higher fraction of absorbing material, and a smaller fraction of diluent in the fuel (in our case ^{238}U) yields more energetic neutron spectra. Consequently, spectrum averaged cross sections for neutron capture in even neutron number nuclides become smaller in outer zones 3-4, and fission to absorption probabilities rise.

The spectrum averaged cross sections for capture and fission in relevant actinides at BOL are displayed in Tables 6 and 7. Note the significant decrease in capture cross sections as median neutron energies increase.

The probability of fission versus capture as a consequence of neutron absorption in a fuel nuclide is of signifi-

Property	zone 1	zone 2	zone 3	zone 4
Pitch/pin ratio	1.95	1.785	1.785	1.785
Fuel pins	331	317	251	319
Absorber pins	0	0	146	78
Technetium pins	0	80	0	0

Table 3: Fuel sub-assembly specification of the lead/bismuth, nitride fuelled Sing Sing Core.

Material	**TRUN**	**UN**	**B_4C**	**Tc**
Zone 1	0.33	0.67	0.00	0.00
Zone 2	0.38	0.42	0.00	0.20
Zone 3	0.63	0.00	0.37	0.00
Zone 4	0.80	0.00	0.20	0.00
Average	0.60	0.18	0.18	0.04

Table 4: Fuel/BA material distributions given as relative volume fractions in each fuel zone.

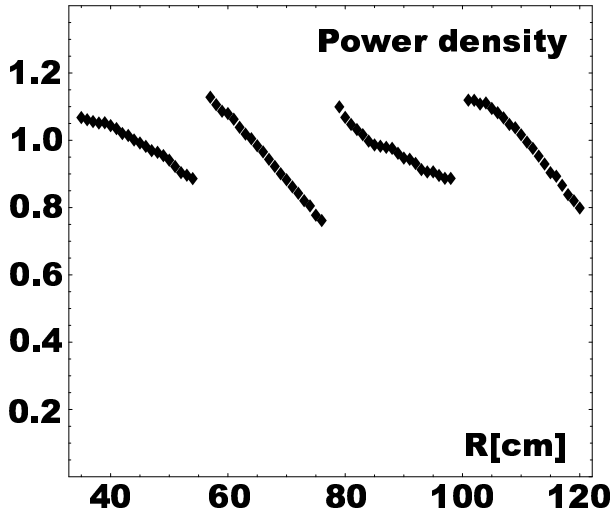

Figure 3: Fission power density at BOL in *fuel* rods along the symmetry axis of the Sing Sing Core. Values are given relative to the core averaged power density. Radial power peaking is seen to be less than 1.2 at a k-eigenvalue equal to 0.972.

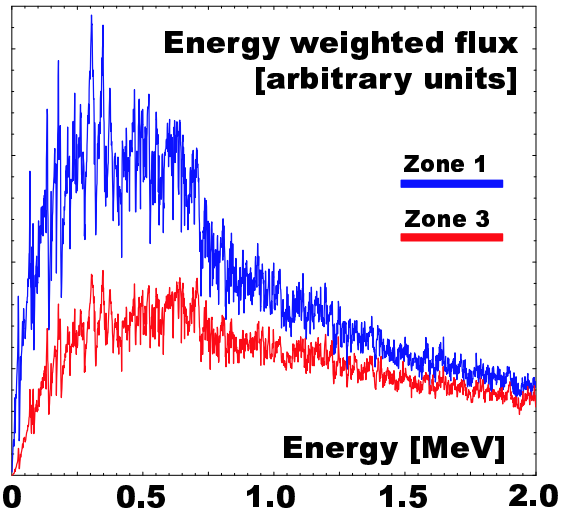

Figure 4: Energy weighted neutron flux spectrum in zone 1 (upper line) and zone 3 (lower line). Neutron capture by ^{10}B in the outer core zones leads to a suppression of flux levels by a factor of more than three in the low energy region ($E_n < 100$ keV).

cance not only for neutron economy, but also for the production of α-emitting nuclides. Formation of ^{242}Cm, having a half life of 163 days, will lead to problems with in-pile fuel swelling and pin pressurization as helium gas is accumulated. The appearance of ^{238}Pu and ^{244}Cm with half lives of 88 and 18 years, respectively, is likely to induce higher costs for reprocessing and fabrication. Thus one would like to maximize fission to absorption probability ratios for predecessors to the quickly decaying α-emitting isotopes. Table 8 displays this ratio for the Sing Sing Core and compares with corresponding values of CAPRA and Energy Amplifier designs [11, 9].

It is remarkable that the fission probability of the even neutron number nuclides is not only dependent on the presence of an absorber, but also the fraction of diluent material in the core appears to play a major role. In the CAPRA core, diluent steel and $^{11}B_4C$ moderator rods are introduced into the fuel assemblies to increase neutron leakage and moderation. In the Energy Amplifier, thorium ($\sim$ 75% volume fraction of fuel) is used to maintain reactivity. Evidently the concomitant neutron moderation through inelastic scattering on thorium eliminates the spectrum hardening benefit of metallic fuel.

Energy	Median	Flux weighted	E > 1 MeV	E > 20 MeV
Zone 1	194 keV	448 keV	10.6%	0.025%
Zone 2	246 keV	522 keV	13.8%	0.007%
Zone 3	356 keV	716 keV	21.8%	0.003%
Zone 4	354 keV	734 keV	22.6%	0.001%

Table 5: Characterization of BOL neutron energy spectrum in the fuel zones of the Sing Sing Core. Note that the contribution of high energy spallation neutrons ($E_n > 20$ MeV) to the total neutron flux at BOL is less than a promille even in the inner fuel zone.

Nuclide	zone 1	zone 2	zone 3	zone 4
^{238}U	0.239	0.193	0.144	0.156
^{237}Np	1.226	0.961	0.663	0.698
^{238}Pu	0.430	0.332	0.228	0.242
^{239}Pu	0.382	0.279	0.183	0.198
^{240}Pu	0.433	0.334	0.234	0.248
^{241}Pu	0.477	0.421	0.362	0.370
^{242}Pu	0.371	0.283	0.193	0.206
^{241}Am	1.604	1.332	1.000	1.029
^{243}Am	1.362	1.089	0.776	0.811
^{244}Cm	0.458	0.383	0.283	0.294
^{245}Cm	0.255	0.199	0.139	0.146

Table 6: One-group cross sections, in units of barn, for neutron capture in the Sing Sing Core fuel zones.

In particular, the increase in fission probability for ^{241}Am from 12% in CAPRA and EA core types to 33% in zone 3 of SSC, points towards a strategy where americium is to be burnt in strongly absorbing fast neutron environments, rather than in moderated targets or diluted cores.

Neutronics

The massive introduction of a non-resonant neutron absorber like boron carbide into a reactor core leads to degradation of reactivity coefficients. Coolant voiding, for instance, increases the probability for fission of even neutron number nuclides. Further, Doppler feedback vanishes, as hardly any neutrons ever reach the resonance region. Table 9 displays values of these important kinetic parameters

Nuclide	zone 1	zone 2	zone 3	zone 4
^{238}U	0.034	0.045	0.073	0.077
^{237}Np	0.346	0.419	0.591	0.600
^{238}Pu	1.133	1.187	1.349	1.359
^{239}Pu	1.714	1.658	1.646	1.663
^{240}Pu	0.400	0.468	0.636	0.646
^{241}Pu	2.236	2.026	1.824	1.859
^{242}Pu	0.282	0.345	0.493	0.501
^{241}Am	0.264	0.329	0.490	0.503
^{243}Am	0.204	0.258	0.392	0.403
^{244}Cm	0.455	0.543	0.753	0.763
^{245}Cm	2.367	2.148	1.962	2.003

Table 7: One-group cross sections, in units of barn, for fission in the Sing Sing Core fuel zones.

for the Pb/Bi cooled Sing Sing Core at BOL. The void worth was calculated by voiding the core (including gaps between sub-assemblies) and upper plena from coolant. The source mode value of the void worth obviously is the physically relevant, but we include the eigenmode void worth in order to enable comparison with deterministic codes. As seen, the advantage of comparatively small void worths (typically less than 1000 pcm, for optimal core designs even negative) of lead/bismuth is partially lost when boron carbide is abundant in the core. A positive value of about +3500 pcm for the present SSC design can be compared with +4500 pcm for JAERI:s sodium cooled ADS design [24].

The Doppler feedback was calculated by exchanging cross sections libraries processed at various temperatures in the core. It was checked that the cross sections used yielded correct temperature behaviour, with *k*-eigenvalue inversely proportional to temperature and Doppler constants in the range of -500 pcm for a simplified model of the CAPRA core [11]. In the very hard spectrum of the Sing Sing Core, however, resonance capture in fuel nuclides is a rare event, and only a small decrease in reactivity with temperature could be observed.

The fraction of delayed neutron emission, β, and the fraction of fissions induced by delayed neutrons, $\beta_{\rm eff}$, were

Nuclide	zone 1	zone 2	zone 3	zone 4	CAPRA	EA
^{237}Np	0.22	0.30	0.47	0.46	0.15	0.15
^{238}Pu	0.72	0.78	0.86	0.85	0.64	0.69
^{240}Pu	0.48	0.58	0.73	0.72	0.37	0.40
^{242}Pu	0.43	0.55	0.72	0.71	0.33	0.32
^{241}Am	0.14	0.20	0.33	0.33	0.12	0.12
^{243}Am	0.13	0.19	0.34	0.33	0.10	0.11
^{244}Cm	0.50	0.59	0.73	0.72	0.40	0.36

Table 8: Fission to absorption probability ratios for quickly decaying α-emitters and their predecessors in the Sing Sing Core fuel zones, compared to corresponding values of CAPRA and Energy Amplifier designs. The benefit of introducing neutron absorbers to reduce α activity and helium accumulation in fuel pins is clear.

Parameter	SSC	CAPRA (1)	CAPRA (2)
Void worth ($k_{\rm eff}$)	+3500 pcm	+1560 pcm	+2210 pcm
Void worth ($k_{\rm S}$)	+4400 pcm		
Doppler constant	-13 pcm	-450 pcm	-400 pcm
β	270 pcm		
$\beta_{\rm eff}$	160 pcm	320 pcm	300 pcm
Neutron life time	0.61 μs	0.84 μs	0.42 μs

Table 9: Kinetic parameters of the Sing Sing Core at BOL, compared to those of the reference CAPRA oxide core (1) and the high burnup CAPRA core featuring minor actinide targets in the reflector (2). Note the unusually small Doppler constant.

calculated by explicitly simulating delayed neutron transport with MCNP4C. The comparatively small value of $\beta_{\rm eff}/\beta \simeq 0.6$ in the Sing Sing Core is due to the low emission energies of delayed neutrons ($\overline{E_{\rm del}} \sim 0.5$ MeV), leading to large probability of absorption in ^{10}B.

A comparison with the kinetic parameters quoted for CAPRA designs [11, 25] shows that the Doppler feedback in case of coolant voiding is very unreliable in the Sing Sing Core, whence subcriticality appears to be a necessary requirement.

Thermal hydraulics

Several important aspects in the thermal hydraulic analysis of accelerator driven system cores differ from those of the classical FBR. Due to the different shape of the power distribution and especially its change over time, one has to be careful in calculating maximum temperatures. Further, with lead/bismuth as a coolant, the lower thermal conductivity will lead to higher temperature gradients within the coolant channel. The range of coolant flow speeds is also more limited for lead/bismuth than for sodium, as erosion of cladding protective oxide films may occur when maximum velocities exceed 3 m/s [18]. Having implemented the oxygen control and monitoring system developed for the russian lead/bismuth cooled submarine reactors [26], in conjunction with use of corrosion resistant, 12Cr-Si ferritic steels, maximum cladding temperatures should kept below 620 degrees C during extended operation [27].

Detailed three dimensional thermal hydraulics simulations of Sing Sing Core coolant flow were performed with StarCD [28], where the Navier-Stokes equation is solved by finite volume modelling employing $k-\varepsilon$ turbulence model. Due to the pronounced turbulent behaviour in near wall regions, wall functions are not applicable to describe the boundary condition between cladding and Pb/Bi coolant. The two-layer model used in the present simulations improves heat friction and heat transfer predictions within the boundary layer, a priori calculating distributions of velocities, temperatures, etc. Heat transfer is implemented through the chemico-thermal enthalpy conservation equations.

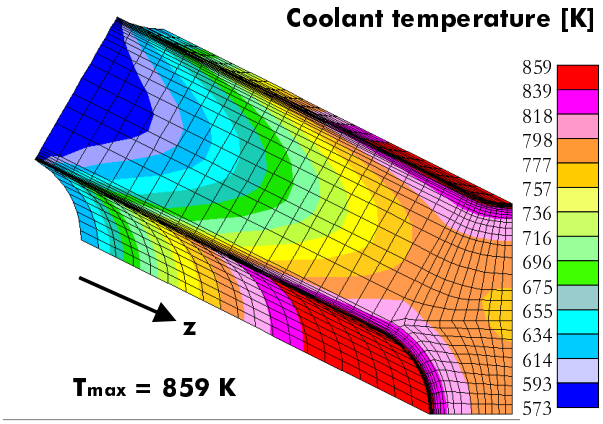

Figure 5: Temperature field in a zone 1 coolant channel, assuming 75 kW of fission power in each fuel pin. Out of this, 7 kW is directly deposited into the coolant by prompt and delayed gamma photons, and by neutrons. An inlet velocity $v = 2.65 m/s$ was adopted in order to keep maximum coolant velocities below $3.0 m/s$.

Pin by pin Monte Carlo simulations showed that the fraction of fission energy deposited directly in the coolant by prompt and delayed gamma photons and neutrons is about nine percent. This effect could be explicitly modelled in StarCD. Similarly, the impact of non-fissile absorber rod presence may be calculated. The resulting coolant temperature field for 75 kW of fission energy release per pin in zone 1 is displayed in Figure 5, for an inlet coolant velocity of 2.65 m/s. A maximum temperature in the interface between coolant and cladding equal to 586 degrees C is found, which is safely below the 620 degrees C limit. The axial temperature rise in the center of the channel is 270 K. The radial temperature gradient increases from about 50 K at the inlet to 120 K at z = 60 cm (where fuel temperatures are maximal). Note that the comparatively low thermal conductivity of lead/bismuth (a factor of six lower than for sodium) leads to higher radial temperature gradients than in typical FBR-channels for identical geometries and coolant velocities.

Thus limits to linear powers in the Sing Sing Core are set to 80 kW per pin in zone 1 and 65 kW in zones 2-4.

Knowing the linear power $\chi(z)$ and temperature profile $T_s(z)$ on the outer pellet surface, maximum fuel temperatures T_i on the inner surface of the pellet can be obtained from standard relations between fuel conductivity, linear power and geometry.

Using the thermal conductivities of actinide nitrides measured by Suzuki and coworkers [29] (The conductivity of AmN was assumed to be $\sim$ 75 % of PuN conductivity) we find that the expressions

$$T_i(z) \simeq T_s(z) + 3.95\chi(z) \text{ kW/(mK)} \quad (1)$$
$$T_i(z) \simeq T_s(z) + 4.61\chi(z) \text{ kW/(mK)} \quad (2)$$
$$T_i(z) \simeq T_s(z) + 5.41\chi(z) \text{ kW/(mK)} \quad (3)$$
$$T_i(z) \simeq T_s(z) + 5.41\chi(z) \text{ kW/(mK)} \quad (4)$$

are approximately valid, for the fuel compositions at BOL in zones 1 to 4, when $T_s < 1000$K and $\chi < 110$ kW/m.

Assuming that nitrogen bonding yields $\Delta T_{\text{gap}} = 1000$ K before gap closure [15], we find that the maximum fuel temperature at BOL is located at about 55 cm height in zone 4 pins closest to the spallation target, being 2100 K for an average core pin power of 44 kW.

In nitrogen atmosphere, decomposition can be suppressed up to T $\simeq$ 2800 K for NpN and PuN [14, 30]. This gives the present core configuration a margin to fuel failure of 700 degrees at BOL. Gap closure at about one percent burnup leads to a temperature decrease of 500 degrees in the pellet. Degradation of bonding conductivity due to release of gaseous fission products will be less severe than in helium bonded pins, especially taking into account that helium produced by α-decaying nuclides is also released in large amounts. Hence, temperature margins will remain larger than 600 degrees until EOL, in spite of the increase in power peaking as burnup proceeds.

Maximum power peaking, and hence maximum burnup is therefore limited by constraints to cladding temperatures, rather than fuel constraints (provided that radiation damage has not yet become unacceptable). The 620 degrees C limit then imposes irradiation to be interrupted before radial power peaking exceeds 1.40 in zone 2 pins, or 1.75 in zone 1 pins.

The issue of decay heat after shut down is less severe for the Sing Sing Core than for typical FBR cores. The larger pin pitches allows for accommodation of a larger heat deposition in the coolant in loss of flow scenarios. Shut down heat due to delayed neutron induced fission is also less by about one third, due to the high probability of delayed neutron absorption in the absorbers. The emission of decay heat was calculated with MCB to be about six percent of full core power at the instant of shut down, going down to one percent within three hours. In any case, cladding melt will occur before fuel temperatures reach the decomposition limit.

Burnup

Limited mainly by cladding temperature constraints a total core power of 1200 MW (including decay heat) was adopted for burnup simulations with MCB. Irradiation was continued without interruption for 300 days, with a 100 day time step where neutron fluxes, power distributions and transmutation rates were recalculated. In order to obtain a sufficient accuracy (one standard deviation less than four percent error in neutron multiplication), the histories of 40 000 neutrons emerging from the spallation target were sampled at each time step. 700 MHz Pentium III double processors running Linux were used for the calculation, yielding time step simulation times of the order of 24 hours. The resulting evolution of k-eigenvalues, required spallation target power, core flux, power peaking and other quantities of interest are summarized in Table 10.

Property	BOL	100 d	200 d	300 d
k-eigenvalue	0.972	0.955	0.936	0.916
ϕ_n^*	0.877	0.870	0.850	0.802
ϕ_f^*	0.875	0.867	0.847	0.797
Target power [MW]	20.5	36.9	54.9	75.1
Power peaking (zone 1)	1.08	1.29	1.49	1.70
Average flux $[10^{19}/(\mathrm{m}^2 \cdot s)]$	3.86	4.14	4.45	4.78
Flux peaking (zone 1)	1.97	2.27	2.57	2.88

Table 10: Evolution of important ADS parameters during 300 days of uninterrupted burnup, imposing a constant thermal power output of 1200 MW. Note that radial power peaking is considerably smaller than radial flux peaking, and stays below 1.75 even at a k-eigenvalue equal to 0.92!

The decrease in k-eigenvalue is 5600 pcm, accompanied by an increase in required spallation target power with a factor of 3.7. The growth in proton beam current is larger than what naively would be inferred from the loss in k-eigenvalue, due to the simultaneous decrease of the source neutron efficiency ϕ_i^*, defined as

$$\phi_i^* \equiv \frac{M_{\mathrm{ext}}^i - 1}{M_{\mathrm{fiss}} - 1} \tag{5}$$

where $M_{\mathrm{fiss}} = 1/(1 - k_{\mathrm{eff}})$ denotes the fundamental mode neutron multiplication. M_{ext}^i describes either the multiplication of the spallation source neutrons according to:

$$M_{\mathrm{ext}}^n = 1 + k_0 + k_0 \cdot k_1 + k_0 \cdot k_1 \cdot k_2 + \cdots \tag{6}$$

where k_0 is the external source neutron multiplication factor, and k_i (i>0) is the generation dependent multiplication factor, or the fission multiplication given by:

$$M_{\mathrm{ext}}^f = 1 + \bar{\nu} N_f \tag{7}$$

where $\bar{\nu}$ is the average number of neutrons released in a fission, and N_f is the number of fissions induced per spallation neutron.

The reasons for the source efficiency being smaller than unity are a larger probability of axial leakage out of the target for spallation neutrons and a relatively large moderation of neutrons within the spallation target, leading to a higher fraction of parasitic capture, than is the case for the average fission neutron. This is a price that is paid for achieving flat power power density, being inevitable if thermal striping of fuel assemblies is to be avoided.

Power peakings remain within the limits set by thermo-hydraulics as discussed above, with neutron fluxes not deviating much from typical FBR-values, except for pins and duct walls closest to the spallation target at EOL. Radiation damage in fuel cladding and ducts is thus not expected to be a problem, since the irradiation time is much shorter than in the typical FBR-cycle.

The transuranium density evolution is exemplified in Figure 6. The core averaged transuranium burnup at end of irradiation is 8.7%, with local burnups ranging from 7.3% in zone 4 to 11.5% in zone 1 and 2.

The higher actinide density is displayed separately in Figure 7. Note that the comparatively higher reduction of higher actinide density in zone 1 (12.2 %) to large extent is due to conversion of ^{241}Am into plutonium via neutron capture and α-decay of quickly decaying curium. As helium accumulation in fuel pins is likely to enhance fuel swelling rates, it would be preferable to burn americium by direct fission rather than by conversion into fissile plutonium. Figures 8 and 9 clearly show the higher densities of these troublesome nuclides appearing in the slower spectrum zones 1 and 2.

Consequently, a refined core design where americium is removed from fuel zones one and two would appear advantageous.

Regarding the reduced TRU transmutation efficiency imposed by the presence of depleted uranium in the inner fuel zones, we note that this is mainly an issue in zone 1, where the slow spectrum leads to a conversion of 5.5% of the present ^{238}U into ^{239}Pu. The corresponding figures for zone 2 is 3.4 % of initial uranium content. As can be seen from figure 6, TRU burnup in zone 1 still reaches 11.5%.

The burnability of ^{10}B is manifested in a 9.3% reduction in boron density in zone 3 and 7.8 % in zone 4. These numbers are larger than the transuranium burnups in each zone, and hence substantiates the proposed role of enriched boron carbide as an efficient burnable poison in a fast spectrum.

Several authors have proposed to use moderated neutron spectra for technetium transmutation [31, 9]. However, as self-shielding will significantly reduce the neutron flux in the center of technetium pins positioned in a thermal or epithermal spectrum [32], fast neutron spectra may perform

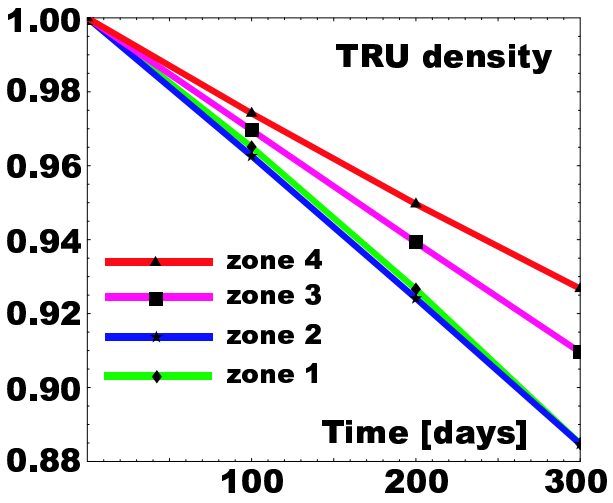

Figure 6: TRU density evolution in the Sing Sing Core operating at 1200 MW thermal power. Values are plotted as fractions of initial nuclide density in the individual fuel zones. A 8.7 % TRU burnup is achieved after 300 full power days.

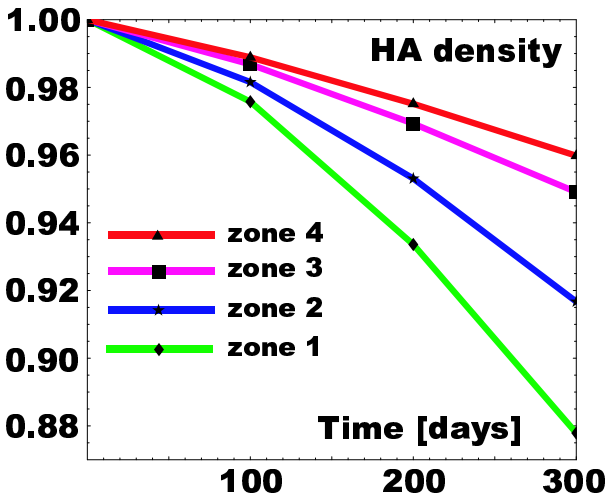

Figure 7: Evolution of higher actinide (americum + curium) density in the Sing Sing Core. The high reduction rate in zone 1 is mainly due to conversion into plutonium following neutron capture in ^{241}Am.

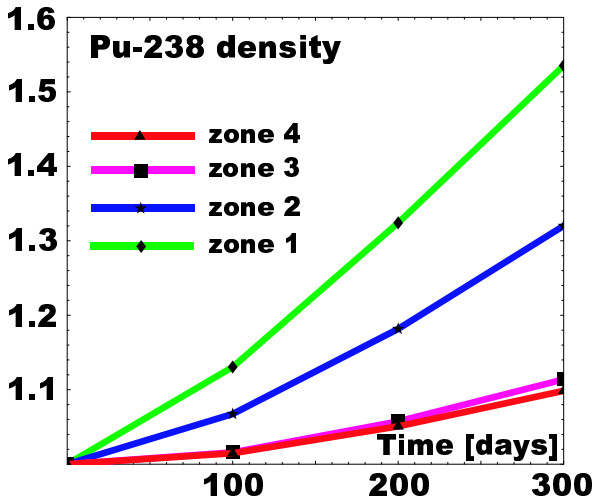

Figure 9: Evolution of ^{238}Pu density in the Sing Sing Core, relative to its initial concentration in each fuel zone. The high growth rate in zone 1 is due to larger capture to fission cross section ratios for neptunium and americium.

equally well. In the present configuration, 4.8% of the 300 kg technetium present in zone 2 is transmuted during the 300 day irradiation period, corresponding to an effective half life of 12 years. Comparing to the 15 year half life obtained in moderated fast reactor assemblies [31], we conclude that fast flux transmutation of ^{99}Tc is at least as efficient.

Conclusions

The introduction of burnable absorbers into sub-critical systems has been shown to have the multifold benefit of flattening power distributions, mitigating reactivity losses, increasing fission to absorption ratios in minor actinides, and lowering helium accumulation in fuel pins. Implementing a four zone differentiation in concentration of enriched boron carbide and depleted uranium we obtained a BOL radial power peaking equal to 1.2 at a *k*-eigenvalue equal to 0.972. Fission to absorption cross section ratios for ^{241}Am as high as 0.33 has been achieved in fuel assemblies where 37 % of the fuel pins had been replaced with absorber pins. Operating the core with a constant thermal power of 1200 MW for 300 days, a transuranium burnup of 8.7% for unrecycled TRU discharges from light water reactors was achieved. As a consequence of the boron introduction, helium accumulation in fuel pins due to formation and decay of ^{242}Cm could be significantly reduced, compared to absorber free core designs like CAPRA and the Energy Amplifier. The concomitant reactivity loss of 640 pcm per percent transuranium burnup in the present core configuration (19 pcm/day) is to be compared to 730 pcm per percent in absorber free cores burning similar TRU compositions. The EOL radial power peaking was 1.70 at a *k*-eigenvalue equal to 0.916, substantially lower than the corresponding flux peaking.

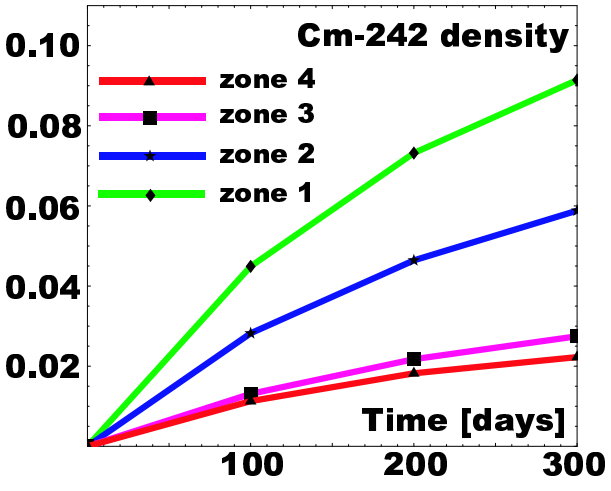

Figure 8: Concentration of ^{242}Cm in the Sing Sing Core, relative to initial ^{241}Am nuclide density in each fuel zone. The significantly lower accumulation rate in outer fuel zones is directly due to the introduction of enriched boron carbide pins in these parts of the core.

The introduction of nitrogen bonding of the fuel pins allows to maintain a margin to nitride decomposition of more than 1000 degrees as linear powers increase up to 77 kW/m in zone 1 at EOL. Measurements of americium nitride stability in nitrogen atmospheres need to be made, however, to verify the assumption made that AmN decomposes at the same temperature as NpN and PuN.

The obvious drawback following upon a massive absorber introduction is a positive void coefficient in conjunction with a minimal Doppler feedback. The choice of lead/bismuth as coolant instead of sodium somewhat mitigates this effect. Reactivity losses are still high enough for

the required spallation target power to rise by more than a factor of three. Such large availability of proton current margin may be a serious safety threat, if accidental insertion of full proton beam power at BOL should occur. These problems, will be addressed in more detailed studies to be performed on the Sing Sing Core in the near future.

Acknowledgements

This work was financially supported by SKB AB (Swedish Nuclear Fuel Ltd), EC (The European Commission), KTC (Centre for Nuclear Technology) and SI (Swedish Institute). The authors would like to thank C. Broeders, F. Venneri and W. Maschek for comments on the use of BA in accelerator driven systems.

References

[1] M. Delpech et al. The Am and Cm transmutation, physics and feasibility. In *International Conference on Future nuclear systems, GLOBAL 99*. ANS, 1999.

[2] S.L. Beaman. Actinide recycle in LMFBRs as a waste management alternative. In *First international conference on nuclear waste transmutation*, page 61. University of Texas, 1980.

[3] H. Murata and T. Mukaiyama. Fission reactor studies in view of reactor waste programs. *Atomkernenergie-Kerntechnik*, 45:23, 1984.

[4] D.G. Foster et al. Review of PNL study on transmutation processing of high level waste. Technical Report LA-UR-74-74, Los Alamos National Laboratory, 1974.

[5] T. Takizuka et al. Conceptual design of transmutation plant. In *Specialist meeting on accelerator driven transmutation technology for radwaste*, page 707. LA-12205-C, Los Alamos National Laboratory, 1991.

[6] M. Salvatores et al. Long-lived radioactive waste transmutation and the role of accelerator driven (hybrid) systems. *Nuclear Instruments and Methods A*, 414:5, 1997.

[7] B. Carluec and P. Anzieau. Proposal for a gas cooled ADS demonstrator. In *International conference on accelerator driven technologies and applications, ADTTA 99*, 1999.

[8] H. Takahashi et al. A fast breeder and incinerator assisted by a proton accelerator. In *Specialist meeting on accelerator driven transmutation technology for radwaste*, page 552. LA-12205-C, Los Alamos National Laboratory, 1991.

[9] C. Rubbia et al. Fast neutron incineration in the energy amplifier as alternative to geologic storage. Technical Report LHC/97-01 (EET), CERN, 1997.

[10] F. Venneri. Disposition of nuclear waste using subcritical accelerator driven systems. Technical Report LA-UR-98-985, Los Alamos National Laboratory, 1998.

[11] A. Languille et al. CAPRA core studies - the oxide reference option. In *International Conference on Future nuclear systems, GLOBAL 95*, page 874. ANS, 1995.

[12] G. Gastaldo, M. Rome, and J.C. Garnier. CAPRA core optimisation by use of $^{11}B_4C$. In *International Conference on Future nuclear systems, GLOBAL 95*, page 1324. ANS, 1995.

[13] H.M. Beaumont et al. CAPRA core studies, high burnup core - conceptual study. In *International Conference on Future nuclear systems, GLOBAL 97*, page 137. ANS, 1997.

[14] H. Matzke. *Science of Advanced LMFBR fuels*. North-Holland, 1986.

[15] M. Mignanelli, R. Thetford, and D. Williams. Fuel performance modelling of nitride fuels. In *International Conference on Future nuclear systems, GLOBAL 99*. ANS, 1999.

[16] H.W. Wiese. Actinide transmutation properties of thermal and fast fission reactors including multiple recycling. *J. Alloys and Compounds*, 271-273:522, 1998.

[17] M. Salvatores, I. Slessarev, and A. Tchistiakov. Analysis of nuclear power transmutation potential at equilibrium. *Nuclear Science and Engineering*, 124:280, 1996.

[18] N. Novikova, Y. Pashkin, and V. Chekunov. Some features of sub-critical blankets cooled with lead-bismuth. In *International conference on accelerator driven technologies and applications, ADTTA 99*, 1999.

[19] R.E. MacFarlane and D.W. Muir. *The NJOY nuclear data processing system, version 91*. LA-12740-M, Los Alamos National Laboratory, 1994.

[20] J.F. Briesmeister. *MCNP - A general Monte Carlo N-Particle transport code, version 4C*. LA-13709-M, Los Alamos National Laboratory, 2000.

[21] M.B. Chadwick et al. Cross section evaluations to 150 MeV for accelerator driven systems and implementation in MCNPX. *Nuclear Science and Engineering*, 131:293, 1999.

[22] J. Cetnar, J. Wallenius, and W. Gudowski. MCB - a continuous energy Monte Carlo Burnup code. In *Fifth international information exchange meeting*, page 523. OECD/NEA, 1998.

[23] J. Cetnar, W. Gudowski, and J. Wallenius. Transmutation calculations with Monte Carlo continuous energy burnup system MCB. In *International conference on accelerator driven technologies and applications, ADTTA 99*, 1999.

[24] T. Takizuka et al. Studies on accelerator driven transmutation systems. In *Fifth international information exchange meeting*, page 383. OECD/NEA, 1998.

[25] H.M. Beaumont et al. Heterogeneous minor actinide recycling in the CAPRA high burnup core with target sub-assemblies. In *International Conference on Future nuclear systems, GLOBAL 99*. ANS, 1999.

[26] B.F. Gromov et al. Use of lead-bismuth in nuclear reactors and accelerator driven systems. *Nuclear Engineering and Design*, 173:207, 1997.

[27] A.E. Rusanov et al. Developing and studying the cladding steels for the fuel elements of the NPIs with heavy coolant. In *Heavy liquid metal coolants in nuclear technology*. IPPE, 1998.

[28] Computational Dynamics Ltd. *Methodology Star-CD version 3.10*, 1999.

[29] Y. Suzuki and Y. Arai. Thermophysical and thermodynamic properties of actinide mononitrides and their solid solutions. *J. Alloys and Compounds*, 271-273:577, 1998.

[30] S. Pillon et al. Preliminary assessment of targets and fuels dedicated to the minor actinides transmutation in the frame of the CADRA program. In *International Conference on Future nuclear systems, GLOBAL 99*. ANS, 1999.

[31] J.L. Kloosterman and J.M. Li. Transmutation of Tc-99 and I-129 in fission reactors. Technical Report ECN-R-95-002, ECN, 1995.

[32] R.J.M. Konings et al. Transmutation of technetium in the Petten high flux reactor. *Nuclear Science and Engineering*, 128:70, 1998.